

## TI Designs: TIDA-01421

# 用于无传感器位置测量的汽车刷式电机纹波计数器参考设计



### 说明

随着现代汽车内小电机的不断改进，为此类电机驱动的座椅、车窗、滑动门、后视镜、后备箱门以及其他部件实现位置记忆存储的需求也在不断增加。现有的解决方案利用连接至电机壳体的多个磁传感器来提供电机控制模块的反馈环路。

无传感器方法为现有解决方案提供了冗余，并且在某些情况下消除了对连接传感器的电机的需求。无传感器方法通过内联电流感应信号调节电路的实现变得越来越流行。本设计为众多控制位置测量的汽车电机系统提供了可轻松修改的解决方案。

### 资源

<a href="#">TIDA-01421</a>	设计文件夹
<a href="#">INA240-Q1</a>	产品文件夹
<a href="#">TLV2316-Q1</a>	产品文件夹
<a href="#">LMV7275-Q1</a>	产品文件夹

### 特性

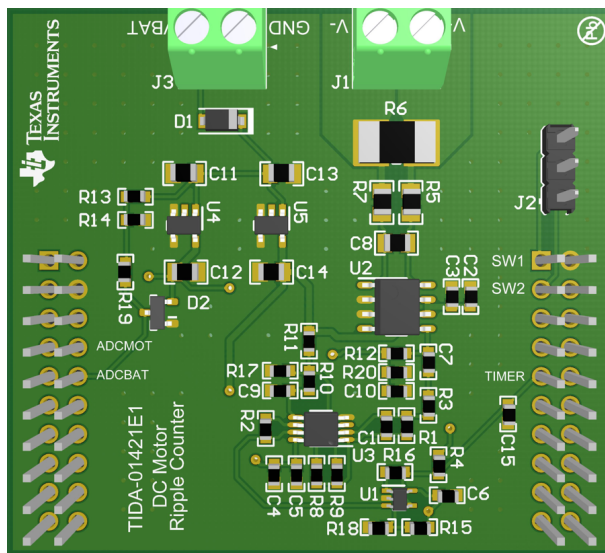
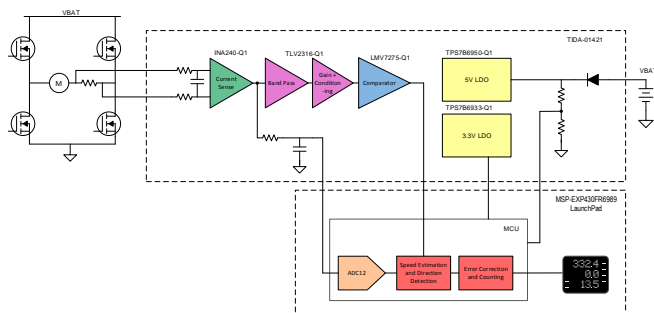
- 可针对多种直流电机解决方案进行配置
- 用于内联电机电流感应的宽共模输入范围
- 可由 9V 至 18V 常用电池电源供电
- 可轻松连接 MSP430™ LaunchPad™ 用于连接和数字捕捉的开发套件
- 高度精确的测试解决方案

### 应用

- [记忆座椅](#)
- [电动车窗](#)
- [后备箱门和电动后备箱](#)
- [侧后视镜](#)



咨询我们的 E2E 专家



该 TI 参考设计末尾的重要声明表述了授权使用、知识产权问题和其他重要的免责声明和信息。

## 1 System Description

Motor position memory is being applied in more areas of the automotive vehicle including configuration and comfort settings for different driver profiles as well as diagnostics for more efficient and smarter control of the motor. The demand for more cost-efficient and easily-configurable solutions for many different motor types has increased. For example, the seats in a vehicle can feature many axes of movement and ergonomic adjustment all controlled by individual motors. Existing memory solutions for these seats require motors with magnetic Hall-effect sensors plus the additional extra wiring for each sensor. Sensorless position measurement reduces the requirement for this many sensors and wiring by sensing the in-line motor current at the seat control module itself.

A sensorless approach is possible for brushed DC motors due to the effect that the back-electromagnetic force (BEMF) has on the motor current seen entering the motor. As the motor rotates, the impedance seen by the BEMF periodically changes due to the nature of the DC motor brushes making contact with multiple poles of the motor and effectively shorting some of the motor windings. This change in impedance changes the measured current in a very periodic pattern proportional to the actual speed of the motor.

This system provides a way to measure this varying in-line motor current, filter and condition the resultant signal, then provide a 3.3-V digital logic level series of rising and falling edges for a digital processor to count and analyze for accuracy and feedback to the main motor controller. With some simple changes in current sense resistor values, gain settings, and filter bandwidths, this solution can quickly be modified for use with many small motor systems.

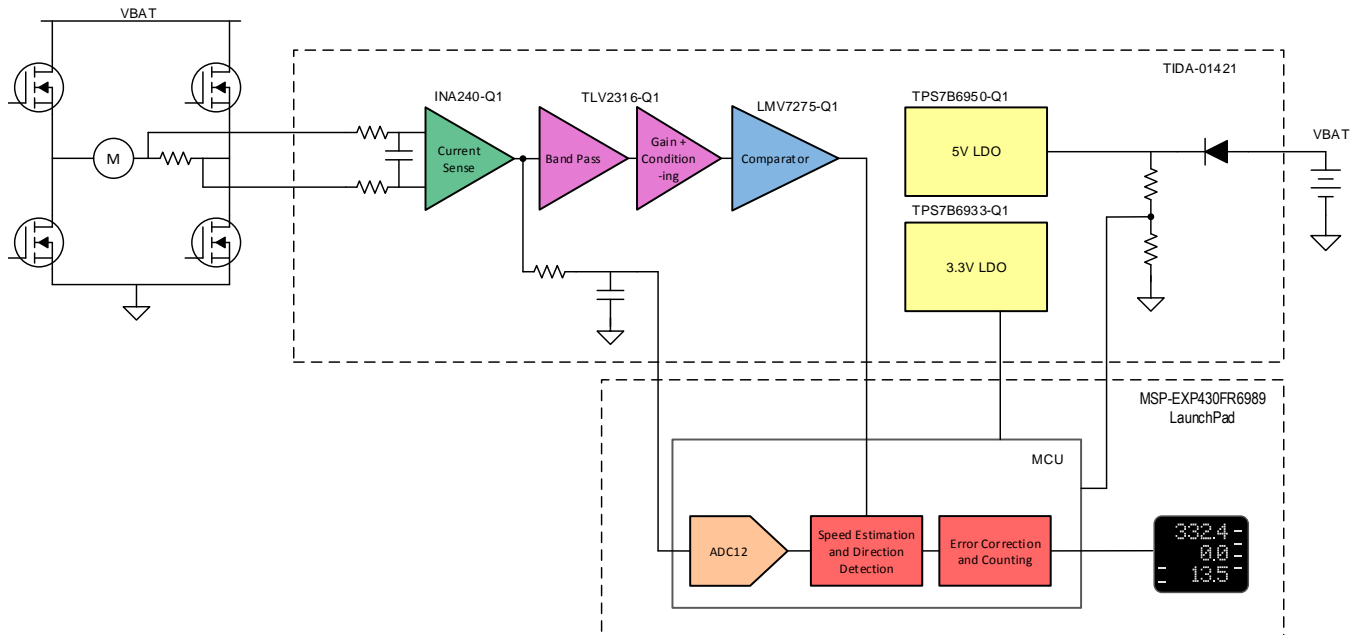
### 1.1 Key System Specifications

表 1. Key System Specifications

PARAMETER	SPECIFICATIONS
Normal power supply operating range	9 V to 18 V
Common mode input range	-4 V to 80 V
Operating ripple frequency range	100 Hz to 1.3 kHz
Maximum motor current	±16 A

## 2 System Overview

### 2.1 Block Diagram



### 2.2 Highlighted Products

#### 2.2.1 INA240-Q1

The INA240-Q1 is a wide common-mode range, high-accuracy, bidirectional current shunt monitor. With a  $-4\text{V}$  to  $80\text{V}$  common-mode range, the device can sense within all typical operating voltage ranges for a DC motor application as well as be protected from typical automotive overvoltage and undervoltage fault conditions. The device features a very large common mode rejection ratio of  $120\text{dB}$ , providing an accurate, low noise measurement even in speed controlled, PWM driven motor solutions. The accuracy and drift performance of this device allow for minimal error when measuring the motor ripples. The device can operate from a single supply from  $2.7\text{V}$  to  $5.5\text{V}$ .

#### 2.2.2 TLV2316-Q1

The TLV2316-Q1 is a dual, low-voltage, rail-to-rail general-purpose operational amplifier. The robust design provides ease-of-use to the circuit designer: a unity-gain stable, integrated radio frequency (RF) and electromagnetic interference (EMI) rejection filter, no phase reversal in overdrive condition, and high electrostatic discharge protection. This dual operational amplifier (op amp) is utilized for the two-stage signal conditioning before the output comparator.

#### 2.2.3 LMV7275-Q1

The LMV7275-Q1 is a single rail-to-rail input low-power comparator and features an open-drain output for correct level shifting to interface with a typical  $3.3\text{V}$  microcontroller (MCU) GPIO. The tiny SC-70 package is ideal for low-voltage, low-power, and space-critical designs.

## 2.2.4 TPS7B69-Q1

The TPS7B69-Q1 is a family of high-voltage, low quiescent current low-dropout linear regulators (LDOs) available in both 3.3-V and 5-V output options. The LDOs power all of the devices on this design, but also provide the necessary 3.3 V to power an MCU.

## 2.3 System Design Theory

The current measured in-line with the brushed motor has both a large-amplitude, very-low frequency DC component and a small-amplitude, high-frequency AC component. Both of these components must be considered when choosing the correct configuration for this design.

The total current seen in-line with the motor can be solved in [公式 1](#) as:

$$I_{\text{MOTOR}} = \frac{(V_{\text{ARMATURE}} - V_{\text{BEMF}})}{R_{\text{ARMATURE}}} \quad (1)$$

where,

- $V_{\text{ARMATURE}}$  is the DC voltage applied across the motor armatures,
- $V_{\text{BEMF}}$  is the BEMF generated by the motor during operation,
- $R_{\text{ARMATURE}}$  is the equivalent series resistance seen between the armatures.

The DC-component current is the main source driving the inductive load of the motor. The motor load varies widely depending on the necessary torque to drive the mechanical motor assembly. In high-torque automotive applications like windows and seats, the steady-state current delivered to these loads can be in the range of 10 A to 20 A.

The AC-component current is created by the sinusoidal BEMF generated by the motor, as well as the periodic changes in motor coil impedance due to the motor brushes shorting adjacent commutator poles. The amplitude and frequency of this component also varies both on the mechanical load on the motor and the design of the motor itself. This AC component contains the ripple that the user should measure and is directly proportional to the actual motor speed. Every ripple corresponds to a commutator pole rotation across the armature brushes. The total sub-divisions of a full rotation can be captured by knowing the total number of poles in the motor.

### 2.3.1 PCB Size and Form Factor

The design includes daughtercard jumpers for connection to an MSP430™ LaunchPad™ to easily interface with an MCU for ripple counting. This requirement is responsible for the necessary 2 in of width on the PCB, after which all other layout considerations were made. The final board design is 2.1 in × 1.9 in after making all the necessary design considerations. The PCB is two-sided and components are only placed on the top side.

The total PCB area is much less in a production design because the large connectors for the battery, in-line motor sense, and the MSP430 LaunchPad jumpers are not necessary. The local linear regulators on the board are likely to be shared with other components on the motor driver controller assembly. The current sense, signal conditioning, comparator devices, and associated passive components on this design were kept as close together as possible to minimize the board space they use, which indicates a typical production-design use case.

### 2.3.2 Current Sense Amplifier Stage

The total motor current can be measured by sensing on the low side of the driver bridge, or in-line with the motor. Sensing current on the low side introduces additional impedances and layout concerns to retain accuracy of the ripple signal. Additionally, to measure ripples in both directions, low-side sensing requires a sensing amplifier on both sides of the full bridge, which increases the total component count. When measuring in-line with the motor, bidirectional measurement with a single device is possible. However, there are design concerns that must be made to ensure an accurate output for the signal conditioning stage.

The MOSFET bridge driving the motor in an automotive application is typically powered directly by the automotive battery. The typical supply range of the battery is 9 V to 14 V; however, some typical automotive conditions can lead to operating voltages of 6 V to 40 V. Note that, when choosing a current sense amplifier, it must be able to withstand common-mode voltages across this entire range to prevent functional damage to the device. The INA240-Q1 has a very-wide common mode range of -4 V to 80 V, which is very capable of withstanding all the possible common-mode conditions expected for the design.

The INA240-Q1 can also be biased to provide a bidirectional output to measure both motor rotational directions. The output stage of the INA240-Q1 utilizes two reference pins, REF1 and REF2, to bias the output. By tying REF2 to the supply voltage V+ and REF1 to ground, the output of the INA240-Q1 rests at the mid-supply rail voltage. In this application, the supply voltage is 5 V; therefore, depending on the motor direction, the output is between 0 V to 2.5 V or 2.5 V to 5 V. This output voltage can be calculated in 公式 2 as:

$$V_{OUT} = I_{MOTOR} \times R_{SENSE} \times GAIN + 2.5 V \tag{2}$$

The maximum current to be sensed can be used to choose the correct value for the sense resistor. For this design, a maximum of 16 A has been chosen. With the INA240-Q1 gain of 50 V/V and 4.9 V as the maximum output voltage,  $R_{SENSE}$  can be solved in 公式 4 by using the previous 公式 2:

$$R_{SENSE} = \frac{(4.9 V - 2.5 V)}{(16 A \times 50 V/V)} = 3 m\Omega \tag{4}$$

The sense resistor must be sized properly for handling a very large amount of power. A size 2512 resistor rated for 3 W has been chosen for this design.

A simple common-mode RC input filter can be used at the input of the INA240-Q1 device to reduce the noise generated by high-frequency motor brush and potential PWM switching noise.

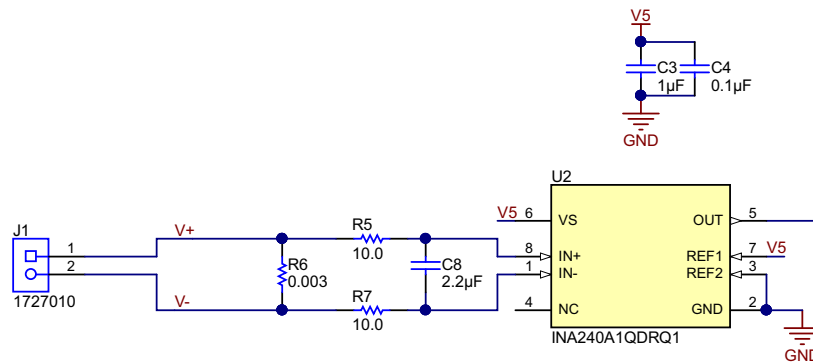


图 1. Schematic of Current Sense Amplifier Stage

### 2.3.3 Band-Pass Filter Stage

The output of the current sense amplifier is filtered with an active band-pass filter to look at the motor ripple signal and remove additional noise and the DC-component variance. The ripple frequency that must be measured largely depends on the typical rotations per minute (RPM) of the motor and the total number of commutator poles. For this design, the filter is limited to about 100 Hz to 1.3 kHz. An inverting amplifier topology has been used to allow for biasing before the next amplifier stage. The simple TLV2316-Q1 has been chosen for its low-voltage operation and rail-to-rail input. Standard op-amp design guidelines pertaining to power supply decoupling and layout considerations are followed.

图 2 shows a schematic of the band-pass filter stage.

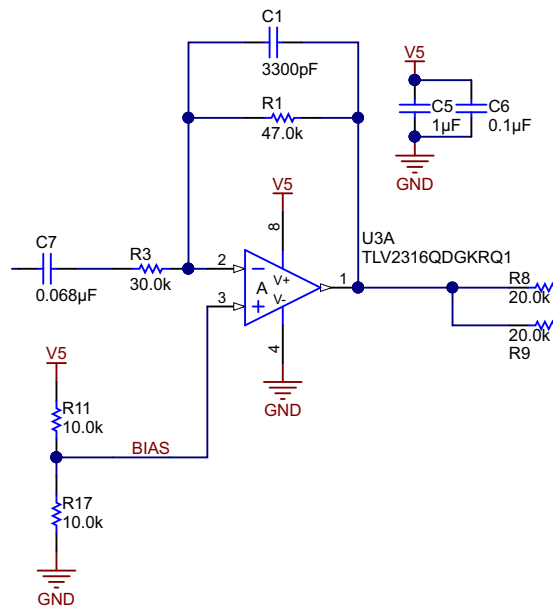


图 2. Schematic of Band-Pass Filter Stage

### 2.3.4 Differential Amplifier for DC-Bias Adjustment

The main goal for the signal conditioning amplifier stages is to generate a clean, low-noise AC signal that can be measured by the final comparator to generate a 0-V to 3.3-V square wave with a switching frequency equal to the motor ripple frequency. Biasing the sinusoidal ripple waveform around the comparator reference point is the preferred method for generating this square wave. The previous filter stage starts this process but the specific filter requirements and operating frequency range lead to some additional necessary steps in the design to ensure proper biasing for the comparator stage.

The high-pass portion of the previous filter stage is configured to approximately 100 Hz, which requires a fairly large RC filter to achieve. This filter also generates a huge time constant that shows its effects on the signal during the very large initial spike in motor current at start-up. This current spike is large enough and slow enough to not be filtered out by the high-pass circuit, and the value for the RC time-constant means that the low-frequency DC component of the signal does not settle to a resting point very quickly. The motor begins to turn during this current spike and ripples are generated. The comparator misses multiple ripples for counting if this change in the effective DC-bias point of the signal is left to remain.

图 3 shows the initial spike in current (yellow waveform) and the resultant signal after the differential amplifier stage (green waveform).

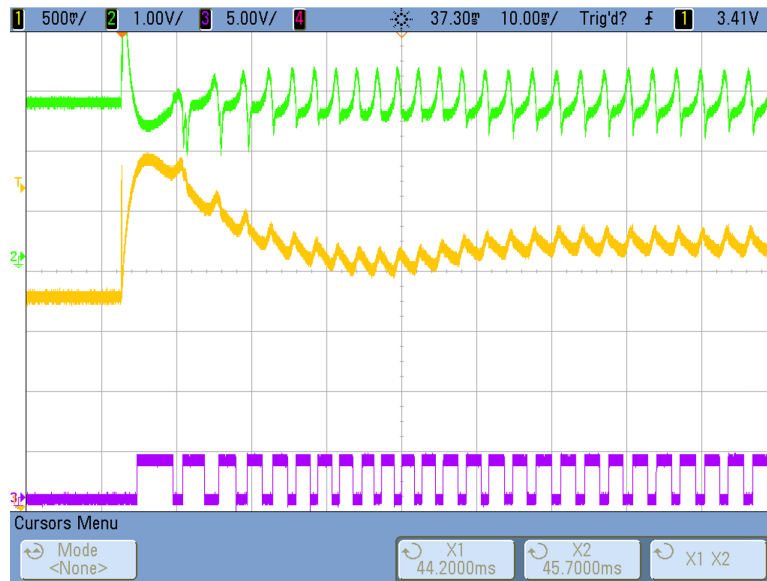


图 3. Oscilloscope Image of Initial Current Spike

This low-speed, high-amplitude current spike is removed from the signal with the unique use of a differential amplifier stage. The output of the band-pass filter is used for both the positive and negative inputs of the amplifier, but one side of the amplifier is very slightly filtered with a low-pass RC filter. This small RC filter causes a very slight phase shift and attenuation of the ripple signal, but has very little effect on the large DC-bias spike. The common mode essentially stays the same on both inputs and is negated by the amplifier. The phase and amplitude difference between the AC signals on both inputs leads to a differential output retaining the ripple frequency component. A very large differential gain of 55 V/V provides a large signal swing of the signal difference and a DC re-biasing around 2.5 V allows the output of this stage to have a very clean and consistent bias point for the signal being measured by the comparator.

图 4 shows the schematic for the differential amplifier stage of the signal chain. The BIAS signal comes from the resistor divider used to bias the previous band-pass filter stage.

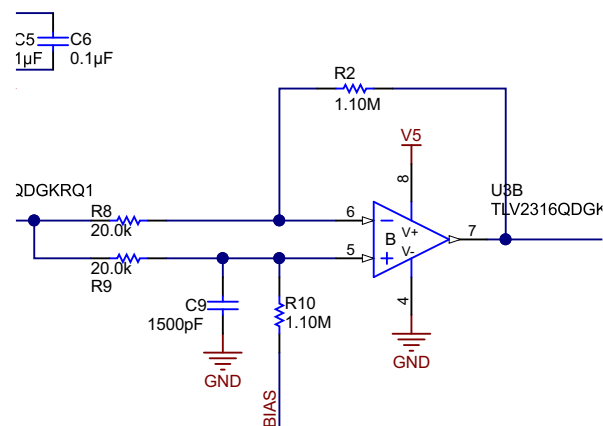


图 4. Schematic of Differential Amplifier Stage

### 2.3.5 Comparator Stage

The comparator stage of the design generates the final 0- to 3.3-V signal used by the MCU for counting. An open-drain output device has been chosen to create the proper 3.3-V levels for input into a typical MCU GPIO. An inverting hysteresis topology (see 图 5) has been utilized to reduce the effects of noise on the input of the comparator.

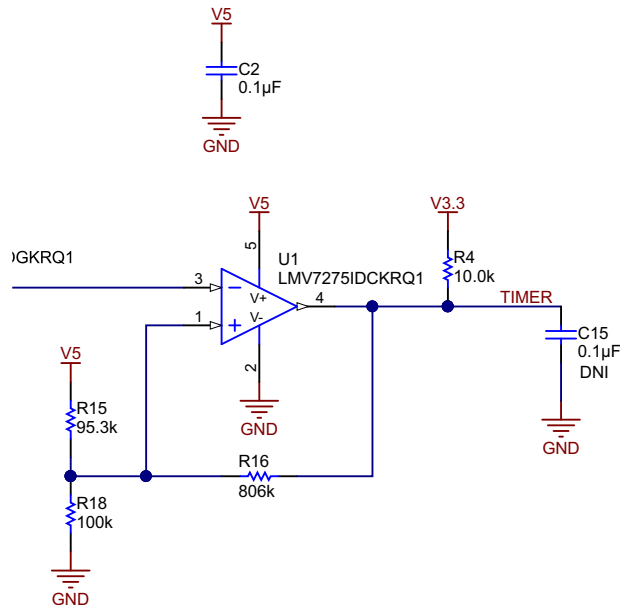


图 5. Schematic of Comparator Stage

For an inverting open-drain topology, the DC thresholds with hysteresis can be determined in 公式 5 and 公式 6 as:

$$V_{TL} = \left( (R_{18} \parallel R_{16}) \times \frac{V_{CC}}{((R_{18} \parallel R_{16}) + R_{15})} \right) + \left( (R_{15} \parallel R_{18}) \times \frac{V_{OL}}{((R_{15} \parallel R_{18}) + R_{16})} \right) \quad (5)$$

$$V_{TH} = \left( (R_{18} \parallel R_{16}) \times \frac{V_{CC}}{((R_{18} \parallel R_{16}) + R_{15})} \right) + \left( (R_{15} \parallel R_{18}) \times \frac{V_{OH}}{((R_{15} \parallel R_{18}) + R_{16})} \right) \quad (6)$$

For this application, the  $V_{OL} = 0$  V causes a slight offset to the centering of the main biasing point for the comparator. Because the AC signal is centered around 2.5 V, the comparator reference point in combination with the feedback resistor is adjusted to allow the  $V_{TL}$  and  $V_{TH}$  to be centered around 2.5 V as well.

### 2.3.6 Motor Power Supply and Current Monitoring

This design includes both the power supply and motor current as the output pin on the LaunchPad jumpers for additional monitoring and control. These pins can be used to recognize faults like overvoltage and overcurrent conditions and can also be used to help correct for errors in the ripple counter.



The battery voltage measures directly after the reverse protection diode. This voltage is then scaled down to meet the input range of a typical 3.3-V MCU. For this design, normal operation is considered 9 V to 18 V, so 18 V is scaled to equal 3 V. Overvoltage conditions can still be monitored up to 19.7 V for the configured voltage divider. Protection diodes and a current limiting resistor have been added on this line to protect the MCU from damage if the battery voltage exceeds 19.7 V. A resistor divider at the output of the current sense amplifier is used to attenuate the signal to meet the maximum 3.3-V input requirements of the MCU ADC.

Assorted mechanical effects on the motor, including brush noise and unusual loading conditions, can cause unwanted effects on the measured signal current. These effects can lead to excessive false or missed triggering of the output comparator. Error correction can be performed in the MCU relying on basic estimations of the motor speed, which are based on the power supply voltage and motor DC current. The motor speed can then be translated to a proportional ripple frequency and compared to the actual ripple frequency. Comparing the estimated ripple frequency to the actual frequency allows for smart error correction of the running ripple count.

Use 公式 7 and the frequency-dependent equation for the BEMF voltage to estimate the motor speed:

$$V_{BEMF} = \omega \times K_e \tag{7}$$

where,

- $\omega$  is the motor speed,
- $K_e$  is the motor constant (taken from the data sheet of the motor).

Replacing  $V_{BEMF}$  in the previous and solving for  $\omega$  leads to 公式 8:

$$\omega = \frac{V_{ARMATURE} - (I_{MOTOR} \times R_{ARMATURE})}{K_e} \tag{8}$$

$R_{ARMATURE}$  and  $K_e$  are known parameters of the motor.  $V_{ARMATURE}$  is the motor supply voltage and  $I_{MOTOR}$  is the motor DC current, which are both values that can be captured by the MCU ADC. The motor current value can also be used to infer the direction of the output for adding or subtracting counts from the total during operation.

图 6 shows the circuitry used to monitor these signals.

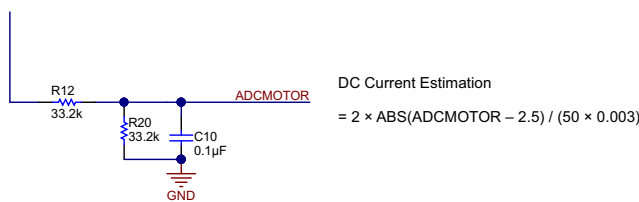


图 6. Schematic of Monitoring Connections (A)

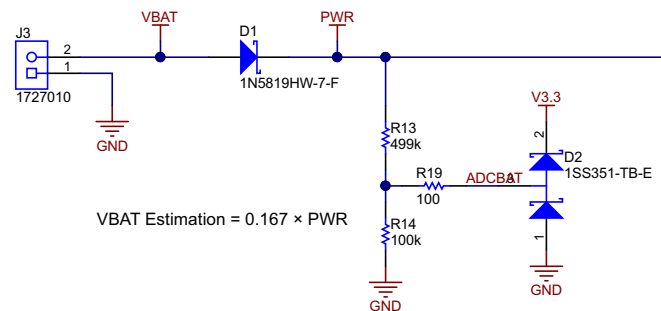


图 7. Schematic of Monitoring Connections (B)

### 2.3.7 3.3-V and 5-V Regulators

This design uses two linear dropout regulators (LDO) for the necessary 3.3- and 5-V voltage supply. These devices have a wide input voltage for operation and protection for the entire possible battery voltage range and all possible fault conditions.

The only design consideration to make for these devices is sizing the capacitors. The data sheet recommends that the input capacitor be larger than 0.1  $\mu\text{F}$  and the output capacitor should be between 2.2  $\mu\text{F}$  and 100  $\mu\text{F}$ . A 4.7- $\mu\text{F}$  value was used as the input capacitor and 2.2  $\mu\text{F}$  was used as an output capacitor on both devices.

图 8 shows the configuration of these LDOs.

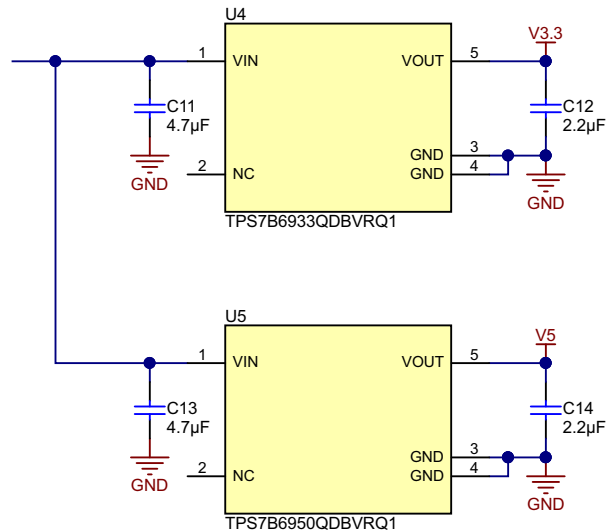


图 8. Schematic of LDO Configuration

### 2.3.8 LaunchPad™ Connectors

To interface with a typical MSP430 Launchpad, the appropriate 20-pin jumpers are used. The following signals are tied to these jumpers:

- 3.3 V for powering the MSP430
- Output of the comparator tied to one of the timer counter pins of the MSP430 for both counting of the ripples and to use the TimerB peripheral to measure the frequency of the ripples for error correction
- Battery supply (ADCBAT) and DC motor current (ADCMOTOR) for both error correction and fault detection
- Two GPIO connections tied to jumper J2 for general purpose use, such as button press signals to detect motor direction

The specific pinout is chosen based on the featured peripherals of the MSP-EXP430FR6989. This board is chosen for very basic functional tests of design from a digital standpoint.

图 9 shows the schematic connections to the LaunchPad jumpers.

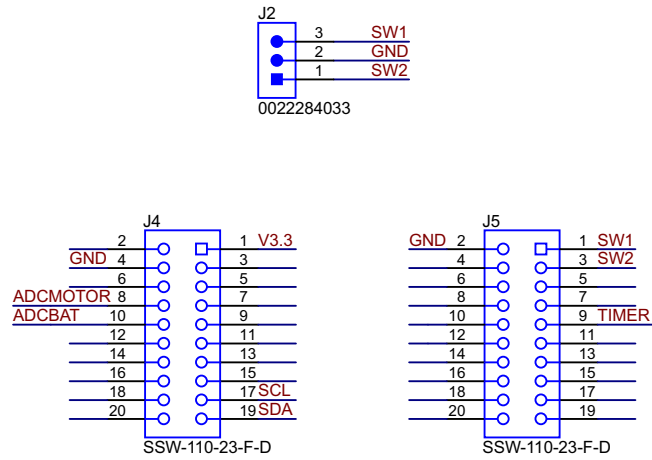


图 9. Schematic of MSP430™ LaunchPad™ Jumper Configuration

### 3 Getting Started Hardware

The larger 20-pin connectors J4 and J7 can interface with a typical MSP430 LaunchPad. The MSP-EXP430FR6989 was used for testing of the design to allow the ripple count to be output to the onboard LCD screen of the LaunchPad.

Jumper J3 provides a connection for a power supply. Jumper J1 is the connection to place the current sense amplifier in-line with the motor. The final jumper, J2, is a simple connection to the LaunchPad GPIOs for button-press detection or other triggering. 表 2 lists details on all the connections.

表 2. Table of all Jumper Connections

JUMPER	PURPOSE
J1	In-line motor current sense connection
J3	Battery power supply connection
J2	MSP430™ GPIO connection for button press, triggering, and so forth
J4, J7	MSP-EXP430FR6989 LaunchPad™ connectors

图 10 shows a rendering of the top side of the PCB and 图 11 shows the PCB attached to the LaunchPad.

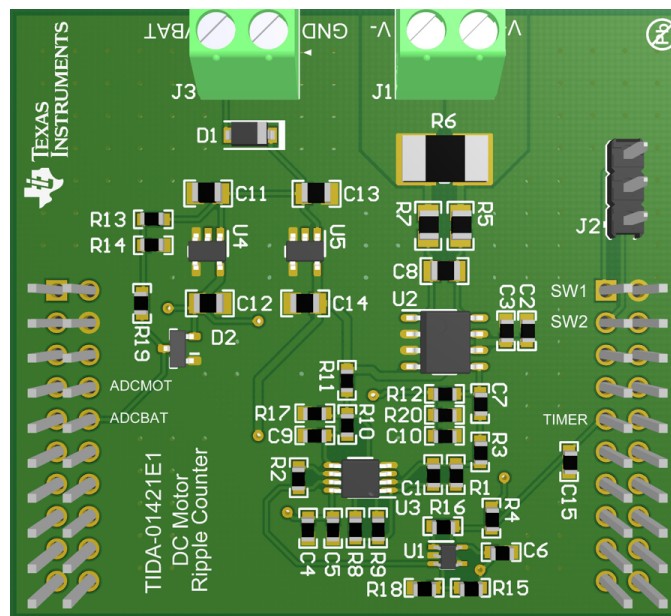


图 10. 3D Rendering of Top Side PCB

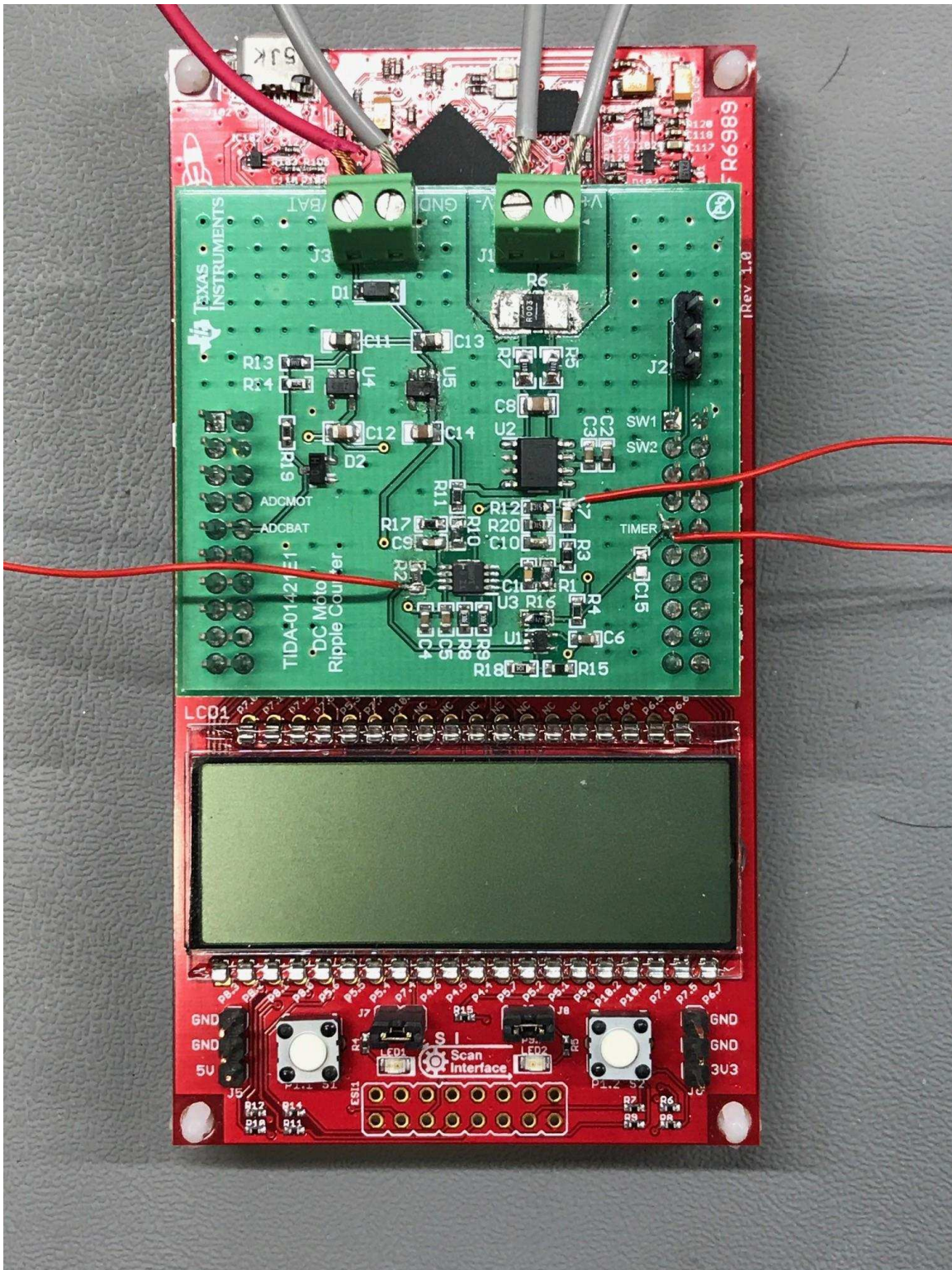
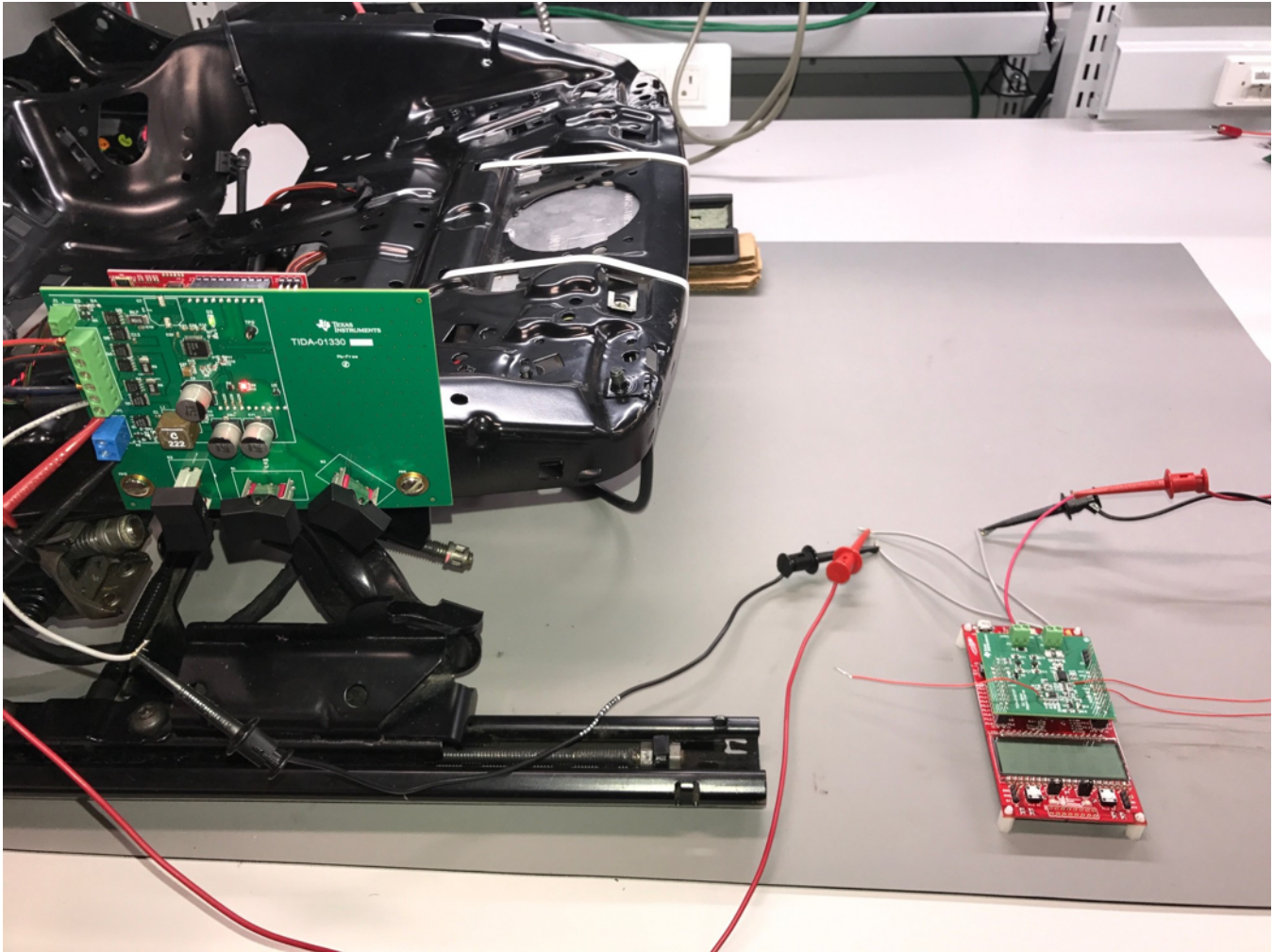


图 11. TIDA-01421 Attached to MSP-EXP430FR6989 LaunchPad™

## 4 Testing and Results

This design was tested in conjunction with the motor driver design of TIDA-01330, a two-axis seat motor driver design. For testing, this board drove the motors on a standard car seat assembly. The ripple counter design was inserted in-line with the motor driver output for both the forward-backward axis as well as the up-down axis motors.



**图 12. Test Setup of TIDA-01421 Tested in Combination of Automotive Seat Assembly and TIDA-01330**

## 4.1 Forward-Backward Motor Operation

In all of the following results, the yellow waveform is the output of the INA240-Q1, the green waveform is the output of the differential-amplifier stage, and the purple waveform is the output of the comparator.

### 4.1.1 Normal Operation at 12 V

The initial tests show the results of the ripple counter when measuring the forward-backward motor at 12 V.

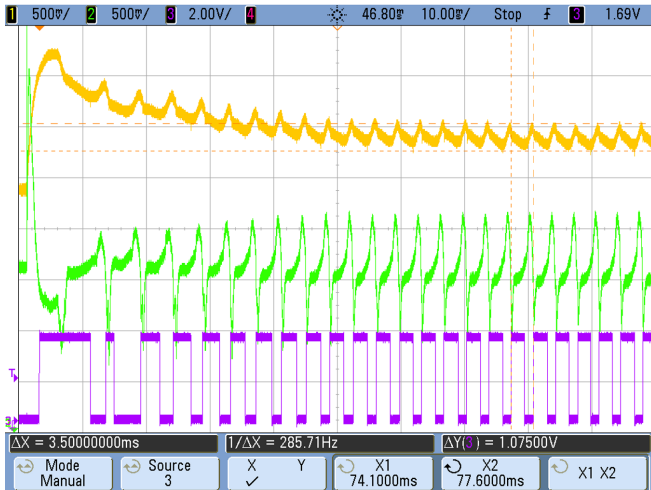


图 13. Forward Motor Operation at 12 V

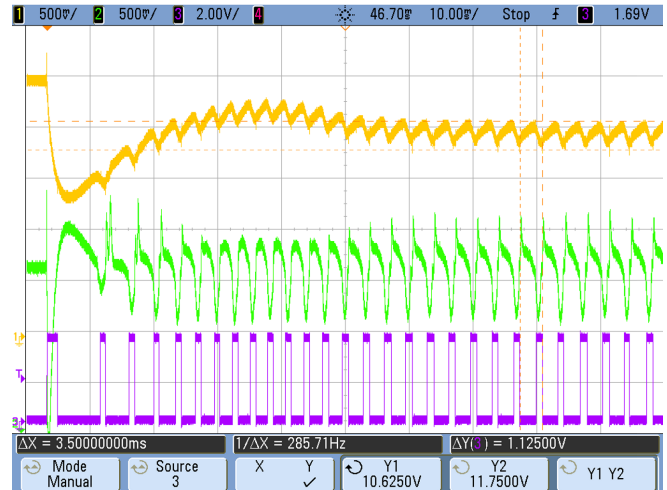


图 14. Backward Motor Operation at 12 V

### 4.1.2 Operation at 9 V and 18 V

The next set of results show the change in motor speed based on a change in the motor supply voltage at 9 V and 18 V.

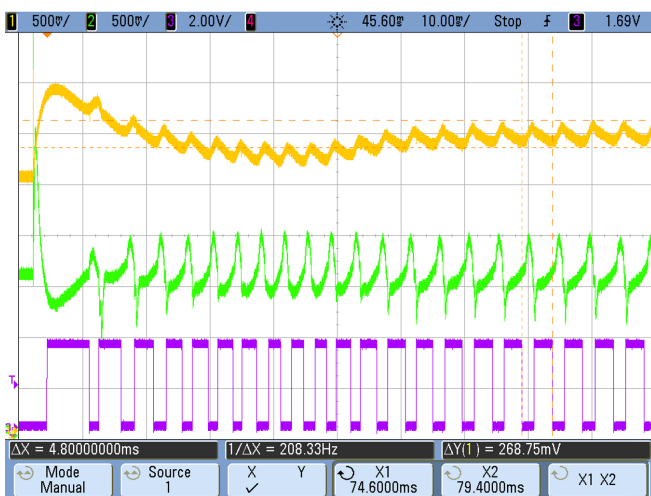


图 15. Forward Motor Operation at 9 V

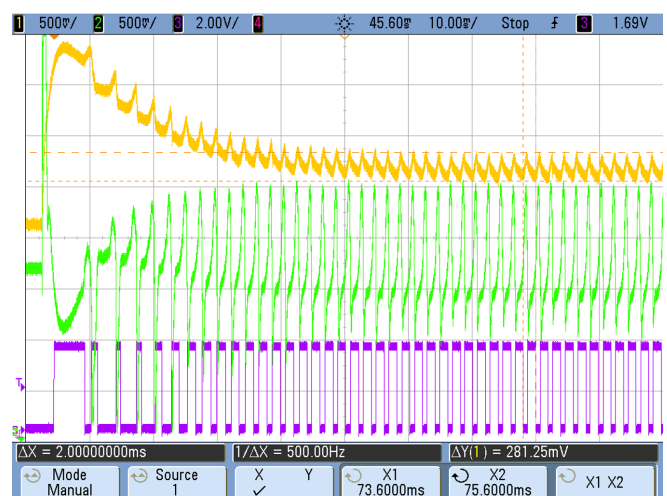


图 16. Forward Motor Operation at 18 V

### 4.1.3 Operation With Added Weight on Seat Assembly

The final set of results show the effects of adding 60 pounds of additional weight on the seat assembly to increase torque on the motor.

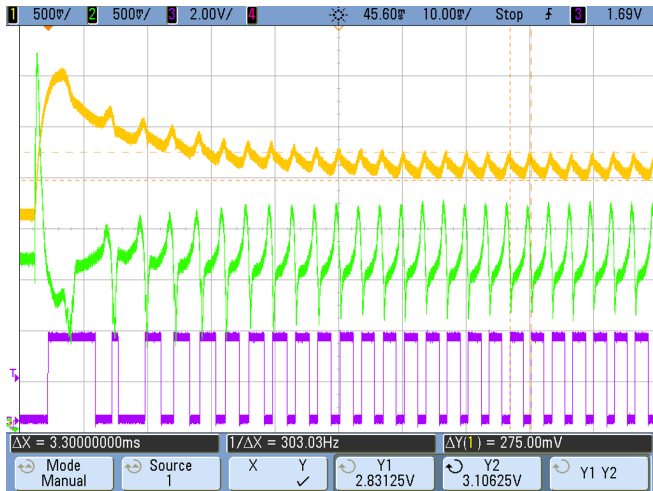


图 17. Forward Motor Operation at 12 V With 60 Pounds of Added Weight

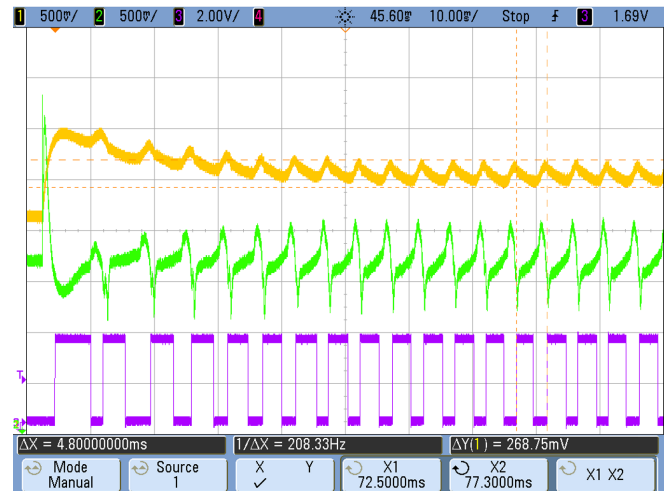


图 18. Forward Motor Operation at 9 V With 60 Pounds of Added Weight

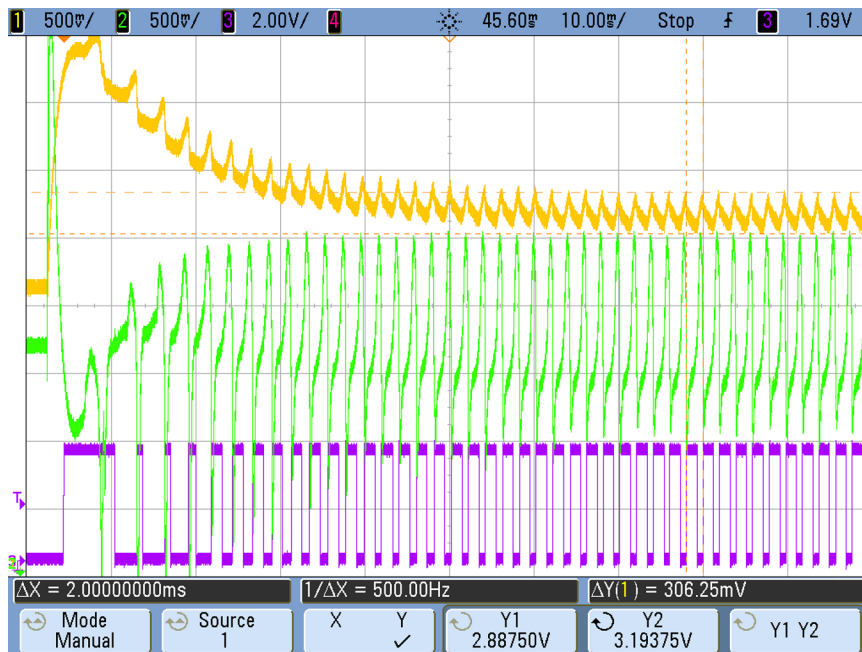


图 19. Forward Motor Operation at 18 V With 60 Pounds of Added Weight



## 4.2 Up-Down Motor Operation

### 4.2.1 Normal 12-V Operation

The initial tests show the performance of the ripple counter when measuring the up-down motor at 12 V.

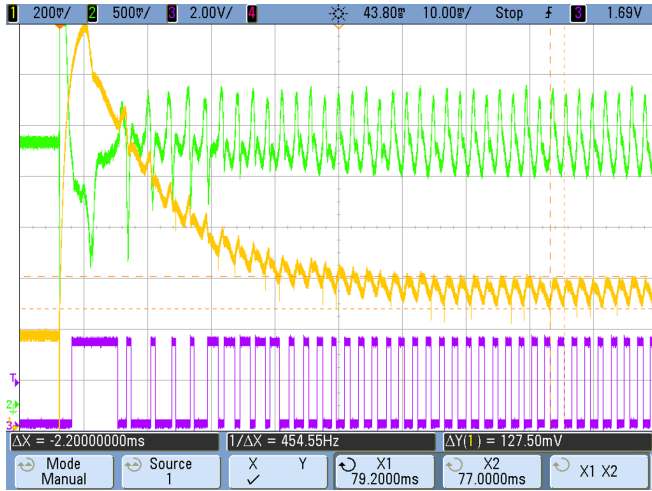


图 20. Upward Motor Operation at 12 V

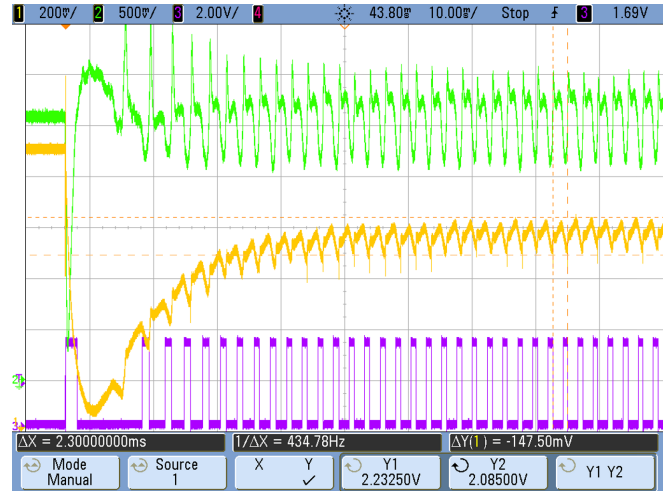


图 21. Downward Motor Operation at 12 V

### 4.2.2 Operation at 9 V and 18 V

The next set of results show the change in motor speed based on a change in motor supply at 9 V and 18 V.

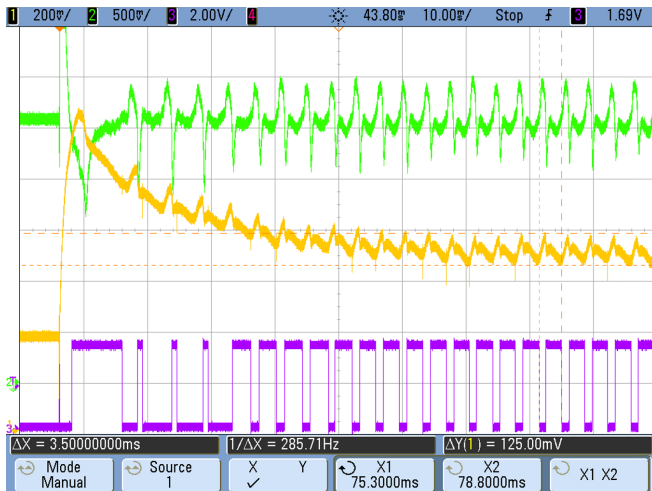


图 22. Upward Motor Operation at 9 V

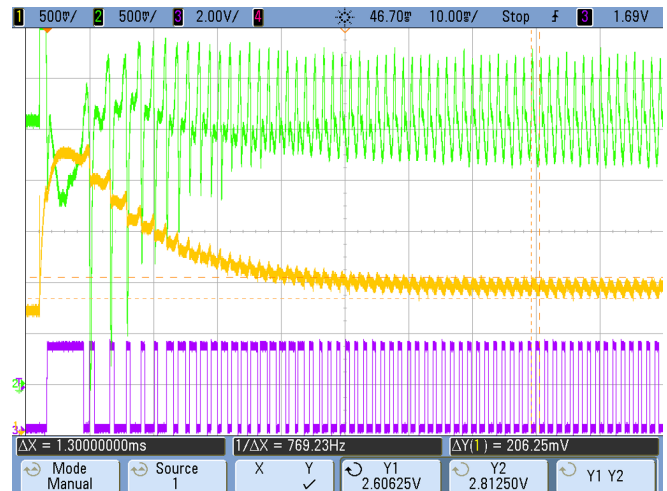


图 23. Upward Motor Operation at 18 V

### 4.2.3 Operation With Added Weight on Seat Assembly

The final set of results show the effects of adding 60 pounds of additional weight on the seat assembly to increase torque on the motor.



图 24. Upward Motor Operation at 12 V With 60 Pounds of Added Weight

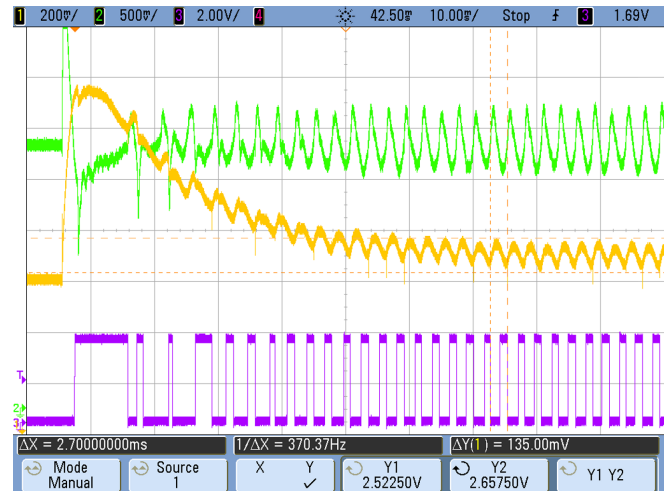


图 25. Upward Motor Operation at 9 V With 60 Pounds of Added Weight

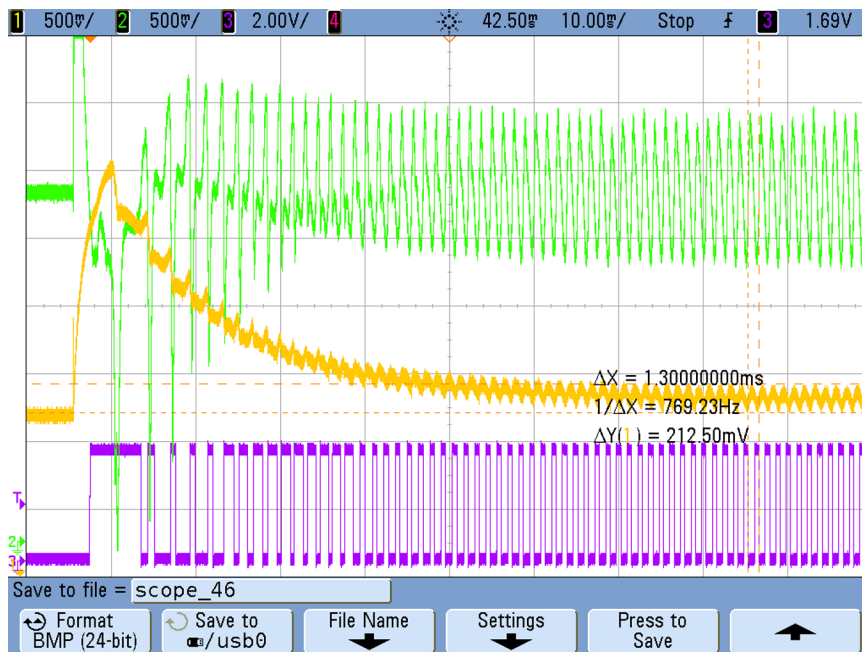


图 26. Upward Motor Operation at 18 V With 60 Pounds of Added Weight

## 5 Design Files

### 5.1 Schematics

To download the schematics, see the design files at [TIDA-01421](#).

### 5.2 Bill of Materials

To download the bill of materials (BOM), see the design files at [TIDA-01421](#).

### 5.3 PCB Layout Recommendations

#### 5.3.1 Layout Prints

To download the layer plots, see the design files at [TIDA-01421](#).

### 5.4 Altium Project

To download the Altium project files, see the design files at [TIDA-01421](#).

### 5.5 Gerber Files

To download the Gerber files, see the design files at [TIDA-01421](#).

### 5.6 Assembly Drawings

To download the assembly drawings, see the design files at [TIDA-01421](#).

## 6 Software Files

To download the software files, see the design files at [TIDA-01421](#).

## 7 商标

MSP430, LaunchPad are trademarks of Texas Instruments.  
All other trademarks are the property of their respective owners.

## 修订历史记录

注：之前版本的页码可能与当前版本有所不同。

<b>Changes from Original (July 2017) to A Revision</b>	<b>Page</b>
• 已更改 all instances of INA282-Q1 to INA240-Q1 .....	<b>3</b>

## 有关 TI 设计信息和资源的重要通知

德州仪器 (TI) 公司提供的技术、应用或其他设计建议、服务或信息，包括但不限于与评估模块有关的参考设计和材料（总称“TI 资源”），旨在帮助设计人员开发整合了 TI 产品的应用；如果您（个人，或如果是代表贵公司，则为贵公司）以任何方式下载、访问或使用了任何特定的 TI 资源，即表示贵方同意仅为该等目标，按照本通知的条款进行使用。

TI 所提供的 TI 资源，并未扩大或以其他方式修改 TI 对 TI 产品的公开适用的质保及质保免责声明；也未导致 TI 承担任何额外的义务或责任。TI 有权对其 TI 资源进行纠正、增强、改进和其他修改。

您理解并同意，在设计应用时应自行实施独立的分析、评价和判断，且应全权负责并确保应用的安全性，以及您的应用（包括应用中使用的 TI 产品）应符合所有适用的法律法规及其他相关要求。就您的应用声明，您具备制订和实施下列保障措施所需的一切必要专业知识，能够 (1) 预见故障的危险后果，(2) 监视故障及其后果，以及 (3) 降低可能导致危险的故障几率并采取适当措施。您同意，在使用或分发包含 TI 产品的任何应用前，您将彻底测试该等应用和该等应用所用 TI 产品的功能而设计。除特定 TI 资源的公开文档中明确列出的测试外，TI 未进行任何其他测试。

您只有在为开发包含该等 TI 资源所列 TI 产品的应用时，才被授权使用、复制和修改任何相关单项 TI 资源。但并未依据禁止反言原则或其他法律授予您任何 TI 知识产权的任何其他明示或默示的许可，也未授予您 TI 或第三方的任何技术或知识产权的许可，该等许可包括但不限于任何专利权、版权、屏蔽作品权或与使用 TI 产品或服务的任何整合、机器制作、流程相关的其他知识产权。涉及或参考了第三方产品或服务的信息不构成使用此类产品或服务的许可或与其相关的保证或认可。使用 TI 资源可能需要您向第三方获得对该等第三方专利或其他知识产权的许可。

TI 资源系“按原样”提供。TI 兹免除对 TI 资源及其使用作出所有其他明确或默示的保证或陈述，包括但不限于对准确性或完整性、产权保证、无屡发故障保证，以及适销性、适合特定用途和不侵犯任何第三方知识产权的任何默认保证。

TI 不负责任何申索，包括但不限于因组合产品所致或与之有关的申索，也不为您辩护或赔偿，即使该等产品组合已列于 TI 资源或其他地方。对因 TI 资源或其使用引起或与之有关的任何实际的、直接的、特殊的、附带的、间接的、惩罚性的、偶发的、从属或惩戒性损害赔偿，不管 TI 是否获悉可能会产生上述损害赔偿，TI 概不负责。

您同意向 TI 及其代表全额赔偿因您不遵守本通知条款和条件而引起的任何损害、费用、损失和/或责任。

本通知适用于 TI 资源。另有其他条款适用于某些类型的材料、TI 产品和服务的使用和采购。这些条款包括但不限于适用于 TI 的半导体产品 (<http://www.ti.com/sc/docs/stdterms.htm>)、[评估模块](http://www.ti.com/sc/docs/sampters.htm)和样品 (<http://www.ti.com/sc/docs/sampters.htm>) 的标准条款。

邮寄地址：上海市浦东新区世纪大道 1568 号中建大厦 32 楼，邮政编码：200122  
Copyright © 2018 德州仪器半导体技术（上海）有限公司